Chapter 4

Study of Emission of Alpha particles in the interaction of ^{14}N with ^{59}Co and ^{93}Nb

Contents

⋆ The work presented in this chapter has been published in a Peer-Reviewed Journal (J. Acharya, S. Mukherjee, *et al.*, Nucl. Phys. A **996**, 121695(2020)) and according to the copyright agreement, the author retains the right to reuse the published work here as a part of this thesis(Elsevier Copyright Policy).

In this work, the results of measured inclusive double differential cross sections of α particles emitted in the interaction of ^{14}N with ^{59}Co and ^{93}Nb at incident energy of 250 MeV are presented. The experimental data were collected in a wide angular range from 8°to 100°in the laboratory system. The analysis of these data suggests that the measured alpha spectra contains contributions of alpha particles originating from various reaction mechanisms, all of which are important at this high energy. We have also compared our experimental results with the calculations by using a recently developed theoretical model code. This recently developed pre-equilibrium model code is hereby put to a stringent test as to how it performs in case of heavy ion reactions at such high energies.

4.1 Introduction

At the projectile energies of 200 MeV and above, heavy ion induced pre-equilibrium emission of nucleons, light charged particles and evaporation residues presents a challenge towards our understanding of physics involving heavy ion reaction mechanism [1]. Efforts have been made in past to identify and predict the reaction cross-section for dominant reaction mechanisms that leads to the emission of nucleons, alpha and other light particles. It is well established that in heavy ion reactions, the compound nucleus mechanism is competing with non-equilibrium and direct reaction processes which are even more dominant at high energies. Experiments have clearly indicated that in such non-equilibrium and direct reactions, alpha particles comprise a major contribution to the emission cross section of all the outgoing particles [2]. Most of these alpha particles originate from projectile break-up [3]. It is possible to separate out and estimate the contributions from direct and evaporation processes from angular distribution and energy spectra. For the case of nucleon emission there are consistent theoretical approaches available which provides a good account of experimental data over a wide range of incident energy and target-mass region [4]. The theoretical model code developed by E. Gadioli, *et al.* [5] was able to predict the contribution of different reaction mechanism involved quite well. There are very few theoretical codes available which addresses the domain of non-equilibrium emission of alpha particles in heavy-ion reactions and give a reasonable account of experimental data obtained over a large incident energy and target-mass range.

In the present work, we aim to investigate about the contribution of direct processes, pre-equilibrium emission and evaporation of particles at such a high incident energy. One of the most widely used code package for simulations of nuclear reaction is TALYS. But it is still a work in progress and doesn't yet have the ability to completely describe heavy ion reactions. Also, the code works well for emission of protons and neutrons but when applied to ^{3}He, alpha particles or heavier ejectiles the results are disappointing [6–8]. Another very promising simulation code is ALICE [9–12] which is based on Monte Carlo simulations of the geometry-dependent hybrid (GDH) model for pre-equilibrium calculations and Weisskopf-Ewing model for the evaporation emission part. It works well at incident energies below 250 MeV, for light as well as heavy incident projectiles. It doesn't take into account the contribution from direct reactions but considers pre-equilibrium emission as well as thermal evap-oration. We have investigated the pre-equilibrium reaction mechanism in the past by studying the excitation functions and neutron emission and have obtained satisfactory results using the version

ALICE2014 [13,14]. But for our current work ALICE2014 under predicts the experimental data by a very large amount, suggesting that there are other possible dominant reaction mechanisms which contribute to the emission of alpha particles at energies presented in this paper.

Recently, a theoretical approach have been developed by O.V. Fotina, *et al.* [15] based on Griffin's model of non-equilibrium processes to describe the spectra of nucleons and other light particles emitted in the non-equilibrium stage of compound nucleus formation. They also took into account the contribution coming from the equilibrium stage of the process within the frame-work of the statistical model. For this purpose the statistical code PACE was modified [16] to accommodate the pre-equilibrium process calculations at sufficiently high energies. It is well known that PACE [17] implements the Hauser–Feshbach formalism to calculate the emission of light particles in the equilibrium stage. Furthermore, the probability of clustering of alpha particles [18–20] inside the projectile was also taken into account to describe the experimental double-differential spectra in a better way.

4.2 Theoretical model

In the Griffin's model of nuclear reactions, the relaxation of the compound nucleus to the equilibrium state is described by the master equation given by:

$$\frac{d}{dt}q(n,t) = \sum_{m=n-2}^{m=n+2} \lambda_{m\to n} q(m,t) - q(m,t)\left(\omega(n) + \sum_{m=n-2}^{m=n+2} \lambda_{n\to m}\right)$$

where $q(n,t)$ is the occupational probability for the composite nucleus state n, $\omega(n)$ is the emission rate of light particles, $\lambda_{m\to n}$ is the internal transition rate. $\lambda_{m\to n}$ nare determined by the matrix elements of the transitions, $\langle |M|^2 \rangle$, and the density of exciton states to which the transition occurs which are in turn determined by single particle level density g. The single particle level density g is related to the level density parameter a ain Fermi gas model by the relation $g = 6a/\pi^2$. Here we have regarded three values as free parameters, the transition matrix element, the single particle level density and the initial exciton configuration. In our case we used initial exciton number as $n_0 = 15(14p, 1h)$. The pre-equilibrium processes have been accommodated in the code for the estimation of double differential cross section. Furthermore, the probable effect of the clustering process of the projectile nucleus on the yield of secondary alpha particles have also been added. The emission of alpha particles at equilibrium was calculated using the Hauser-Feshbach formalism as included in the PACE code. A detailed theoretical description of the model can be found in O.V. Fotina, *et al.* [15].

4.3 Experimental Details

The experiment was performed at the cyclotron facility of the iThemba LABS, Somerset West, South Africa, where the beam of ^{14}N ions of 250 MeV energy was supplied. A detailed description of the facility can be found in J.V. Pilcher, *et al.* [21]. The beams were focused on the target mounted at the centre of a 1.5 m diameter scattering chamber. The targets were mounted in aluminium frames with 25 mm diameter apertures. The ^{93}Nb and ^{59}Co target thicknesses were 1.72 mg/cm^2 and 1.00 mg/cm^2, respectively. A set of two $\Delta E - E$ Si surface-barrier detectors were used for particle identification, whose thicknesses were selected in such a way so as to cover both a lower and a higher energy region. One telescopes had thicknesses of 30 μm and 500 μm while the other had thicknesses of 100 μm and 2000 μm, respectively. Both detectors were mounted on two rotatable arms inside the scattering chamber on opposite sides of the beam and in the same reaction plane. By combining the data from both the telescopes, complete en-ergy spectra was obtained. Other details of the detector arrangement and electronics used in the experiment can be found in the paper of another similar type of experiment performed here [5]. Data were acquired at various scattering angles ranging from 8°- 120°. The overall systematic uncertainty of the absolute cross section values is estimated to be less than 10%.

4.4 Results and Discussion

Figs. 4.1 and 4.2 show energy spectra of alpha particles at various angles in the reaction of ^{14}N with ^{59}Co and ^{93}Nb at an incident energy of 250 MeV. It can be seen that at very forward angles (8°- 15°) the cross-section remains almost constant between 40 MeV to 80 MeV, while for alpha-particles emitted with energies above 80 MeV, there is a rapid decrease in the cross-section as the energy increases. But at higher angles there is no such type of constant region and the cross-section keeps on decreasing rapidly with alpha particle energy right from the start. This trend is seen because of the spectator alpha particles, which are produced in the breakup of the projectile, and whose contribution decreases very rapidly at relatively larger angles (> 20°) as seen in the literature [22, 23]. It is these spectator alphas which are responsible for high energy tail.

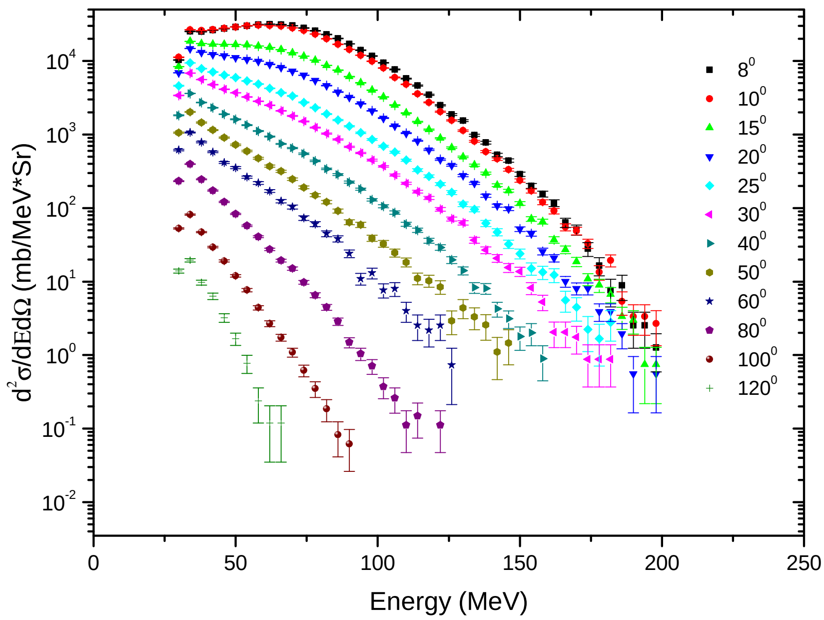

Figure 4.1: Experimental double differential α-particle spectra for the interaction of ^{14}N with ^{59}Co at incident energy of 250 MeV.

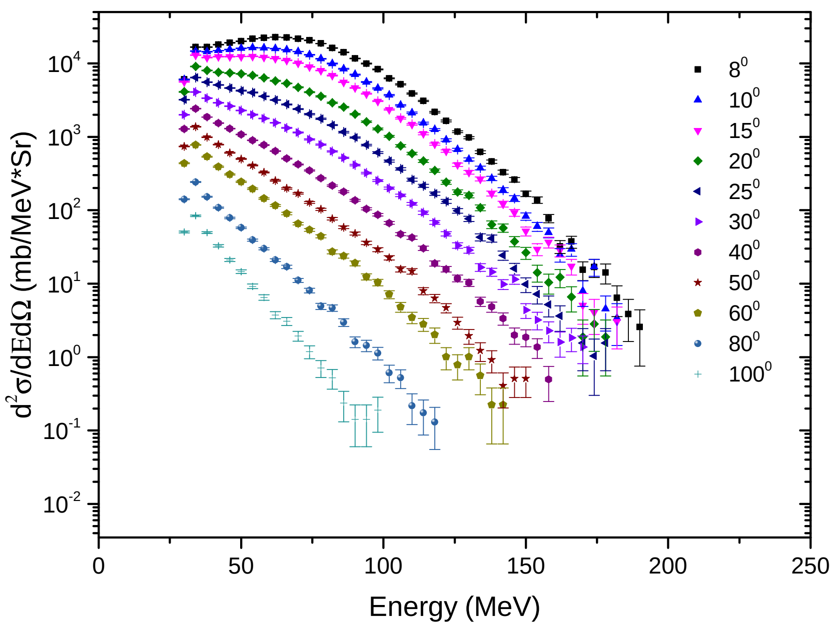

Figure 4.2: Experimental double differential α-particle spectra for the interaction of ^{14}N with ^{93}Nb at incident energy of 250 MeV.

The "flat" region of the low energy alphas in the forward angle curves can be said to have majority of contribution from alphas which are re-emitted with reduced energy after undergoing incomplete fusion. These are created in the breakup of the projectile and, at incident energy used in present study and higher, there are high chances that they will not get dissociated immediately in the target nucleus after fusion and will survive for a few interactions with the nucleons and will get re-emitted with reduced energy in the forward cone. Results indicates that there is $\sim$ 50-70% decrease in energy of alpha particles after the fusion, when they are re-emitted. As we go towards higher angles, it is seen that the contribution of alpha particles coming from break-up decreases drastically and re-emission and pre-equilibrium emission becomes dominant mode of emission.

As shown in Figs. 3 and 4 we have compared our experimental results for ^{59}Co target with the modified PACE code which takes into account equilibrium and pre-equilibrium processes. At forward angles (15°and 25°) there is a large underestimation by the code as in this region the contribution from direct reactions are very much dominant. But as we go towards higher angles (above 40°) this underestimation reduces, as the contributions from direct reaction decreases and pre-equilibrium emission become the dominant modes of alpha particle emission within the range of 40°to 80°.

At even larger angles (backward angles) the contribution of pre-equilibrium alpha particles also becomes negligible as mostly only emission from the equilibrium state persists.

Figs. 4.5 and 4.6 show the comparison of experimental data with predictions by the modified PACE code for the ^{93}Nb target at various angles. These spectra show asimilar trend as that of ^{59}Co. The dominant alpha emission mechanism in various regions is same as that in the case of ^{59}Co.

Fig.4.7 shows the angular distribution of alpha particles for various emission energies. It can be seen that alpha particles with energies more than 150 MeV are not emitted at emission angle more than $\sim$50°. As the emission energy increases the angular distribution becomes more and more forward peaked. In the emission region below 150 MeV, re-emission after incomplete fusion, pre-equilibrium and evaporation emissions becomes dominant mode of emission. Majority ($\sim$90 %) of alpha particles emitted have relatively low energies (below 90 MeV) which means pre-equilibrium and evaporation mechanism are the major contributors to the emission of alpha particles as compared to direct processes.

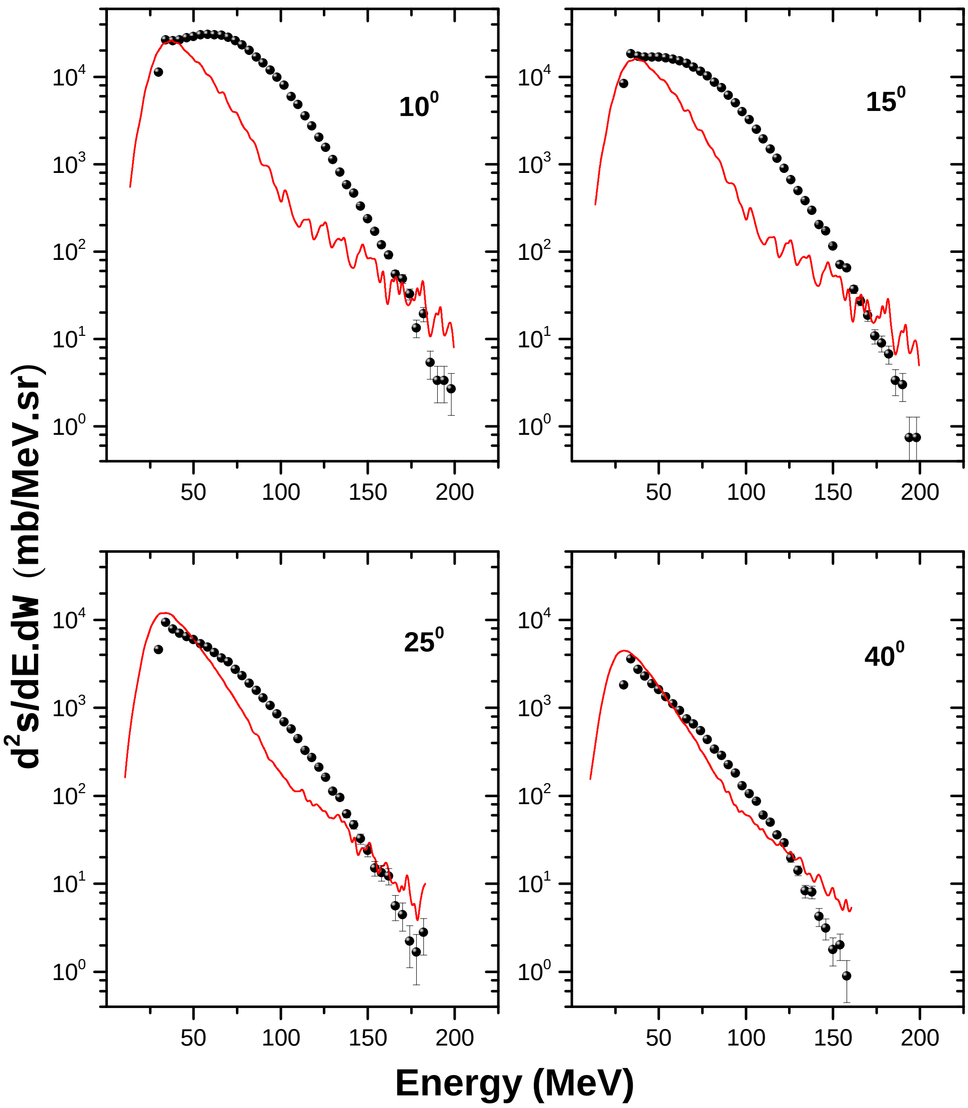

Figure 4.3: Comparison between experimental and theoretical double differential α-particle energy spectra for the interaction of ^{14}N with ^{59}Co at an incident energy of 250 MeV at various angles. Solid spheres (black) are experimental data points which include error bars and the results of modified PACE4 are shown as solid curve (red).

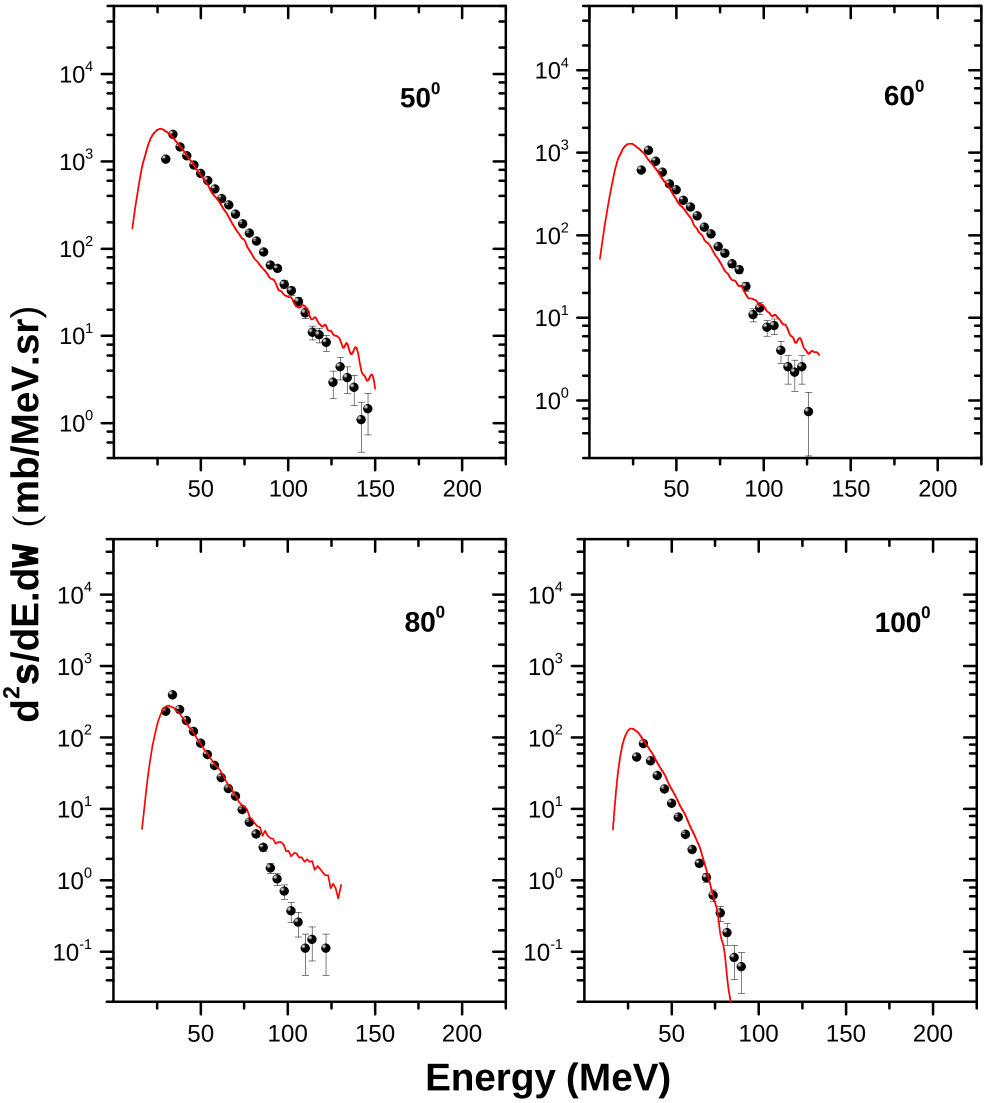

Figure 4.4: Comparison between present experimental double differential α-particle energy spectra for the interaction of ^{14}N with ^{59}Co at 250 MeV (solid symbols) and modified PACE4 (solid lines).

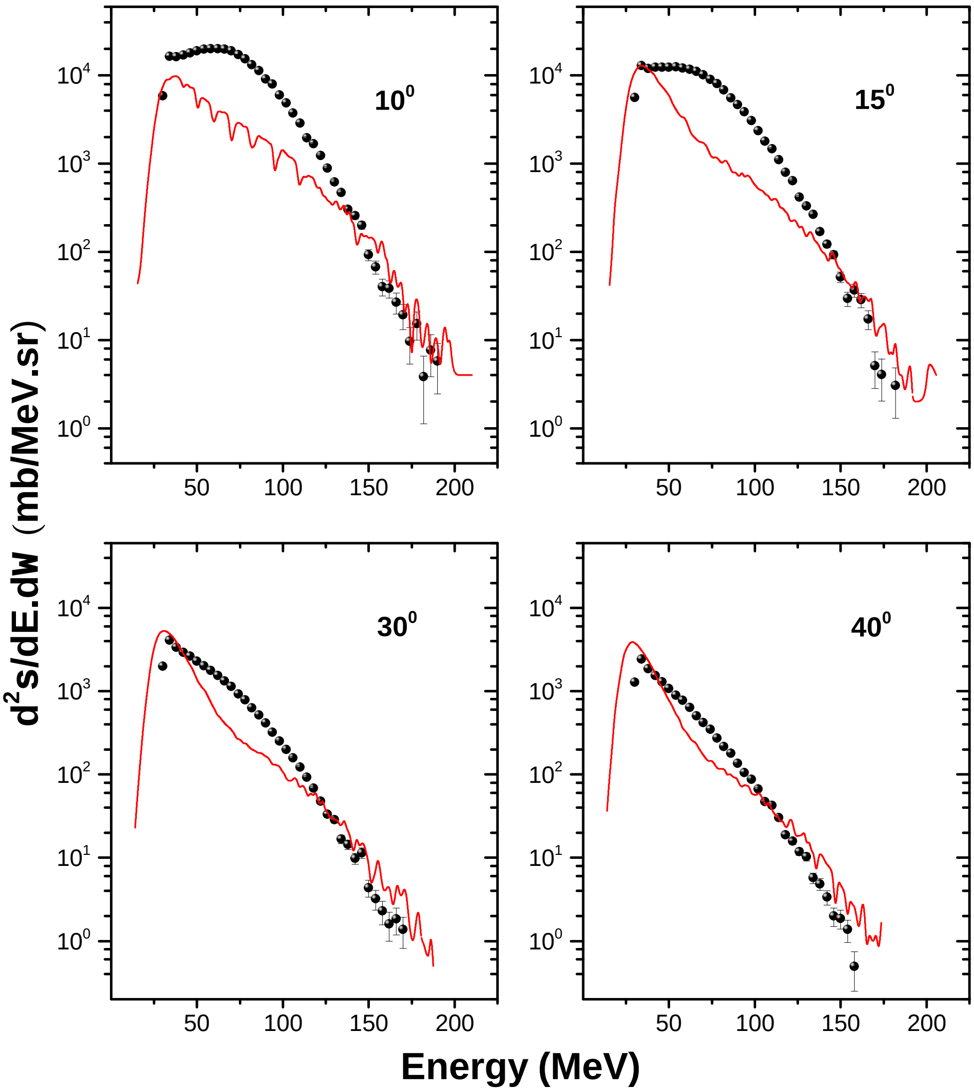

Figure 4.5: Comparison between experimental and theoretical double differential α-particle energy spectra for the interaction of ^{14}N with ^{93}Nb at an incident energy of 250 MeV at various angles. Solid spheres (black) are experimental data points which include error bars and the results of modified PACE4 are shown as solid curve (red).

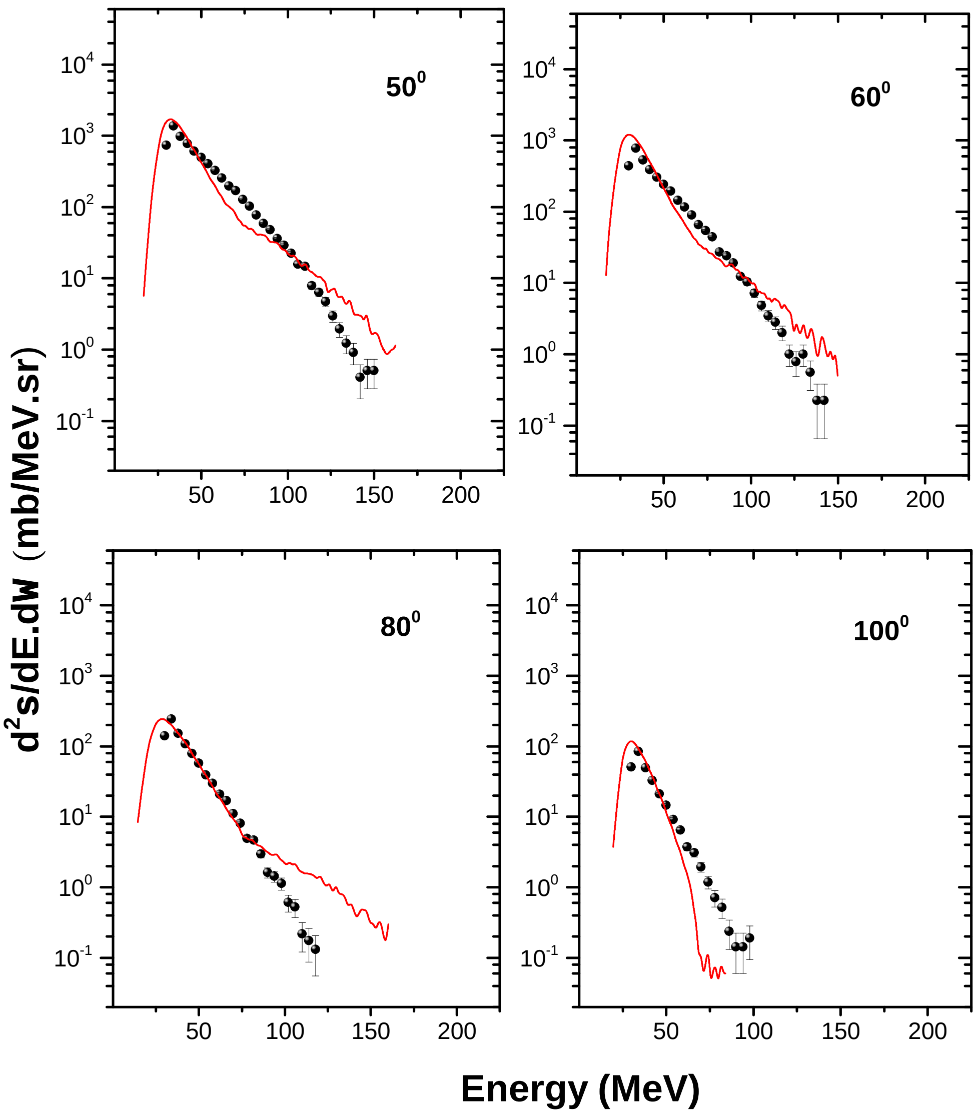

Figure 4.6: Comparison between present experimental double differential α-particle energy spectra for the interaction of ^{14}N with ^{93}Nb at at 250 MeV (solid symbols) and modified PACE4 (solid lines).

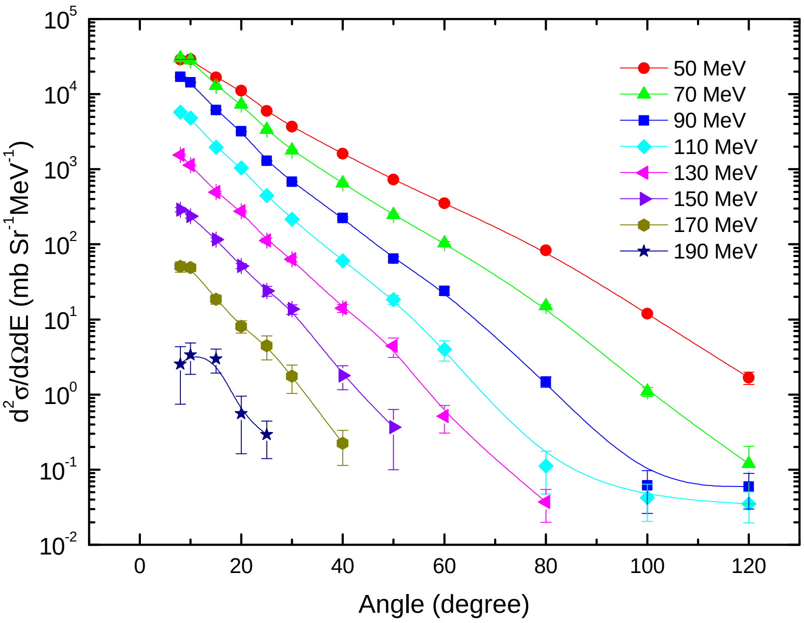

Figure 4.7: Experimental angular distribution of α-particles emitted in the interaction of ^{14}N with ^{59}Co at 250 MeV.

✠ ✠ ✠ ✠

Bibliography

[1] D.S. Ginger, K. Kwiatkowski, G. Wang, W.C. Hsi, S. Hudan, E. Cornell, R.T. de Souza, V.E. Viola and R.G. Korteling, Phys. Rev. C **78**, 034601 (2008).

[2] H.C. Britt and A.R. Quinton, Phys. Rev. **124**, 877 (1961).

[3] K. Siwek-Wilczynska, E.H. du Marchie van Voorthuysen, J. van Popta, R.H. Siemssen and J. Wilczynski, Nucl. Phys. A **330**, 150 (1979).

[4] E. Gadioli and P.E. Hodgson, Pre-Equilibrium Nuclear Reactions, Oxford University Press, New York, 1992.

[5] E. Gadioli, M. Cavinato, E. Fabrici, E. Gadioli Erba, C. Birattari, I. Mica, S. Solia, G.F. Steyn, S.V. Förtsch, J.J. Lawrie, F.M. Nortier, T.G. Stevens, S.H. Connell, J.P.F. Sellschop and A.A. Cowley, Nucl. Phys. A **654**, 523 (1999).

[6] R. Bevilacqua, PhD Thesis, Uppsala University, 2011.

[7] A.A. Cowley, G.J. Arendse, J.W. Koen, W.A. Richter, J.A. Stander, G.F. Steyn, P. Demetriou, P.E. Hodgson and Y. Watanabe, Phys. Rev. C **54**, 778 (1996).

[8] A. Budzanowski, M. Fidelus, D. Filges, F. Goldenbaum, H. Hodde, L. Jarczyk, B. Kamys, M. Kistryn, St. Kistryn, St. Kliczewski, A. Kowalczyk, E. Kozik, P. Kulessa, H. Machner, A. Magiera, B. Piskor-Ignatowicz, K. Pysz, Z. Rudy, R. Siudak, M. Wojciechowski, Phys. Rev. C **80**, 054604 (2009).

[9] M. Blann, Phys. Rev. C **54**, 1341 (1996).

[10] M. Blann and M.B. Chadwick, Phys. Rev. C **57**, 233 (1998).

[11] M. Blann and M.B. Chadwick, Phys. Rev. C **62**, 034604 (2000).

[12] M. Blann, A.Y. Konobeev, Pre-compound cluster decay in HMSALICE, available in documentation supplied with RSICC code package PSR-550

(package name ALICE 2014/ALICE 2017), https://rsicc .ornl .gov /codes /psr /psr5 /psr-550 .html(unpublished).

[13] J. Acharya, S. Mukherjee, G.F. Steyn, N.L. Singh and A. Chatterjee, Phys. Rev. C **93**, 024608(2016).

[14] J. Acharya, S. Mukherjee, A. Chatterjee and N.L. Singh, Phys. Rev. C **97**, 034607 (2018).

[15] O.V. Fotina, D.O. Eremenko, Yu.L. Parfenova, S.Yu. Platonov, O.A. Yuminov, V.L. Kravchuk, F. Gramegna, S. Barlini, G. Casini, M. Bruno, M. D'Agostino, O. Wieland, A. Bracco and F. Camera, Int. J. Mod. Phys. E **19**, 1134 (2010).

[16] I.M. Egorova, S.O. Eremenko, S.Yu. Platonov, O.V. Fotina and O.A. Yuminov, Bull. Russ. Acad. Sci. Phys. **66**, 1622 (2002).

[17] A. Gavron, Phys. Rev. C **21**, 230 (1980).

[18] O.V. Fotina, S.A. Goncharov, D.O. Eremenko, S.Yu. Platonov, O.A. Yuminov, V.L. Kravchuk, F. Gramegna, T. Marchi, M. Cinausero, M. D'Agostino, M. Bruno, G. Baiocco, L. Morelli, M. Degerlier, G. Casini, S. Barlini, S. Valdrè, S. Piantelli, G. Pasquali, A. Bracco, F. Camera, O. Wieland, G. Benzoni, N. Blasi, A. Giaz, A. Corsi and D. Fabris, EPJ Web Conf. **66**, 03028 (2014).

[19] D. Fabris, F. Gramegna, T. Marchi, M. Degerlier, O.V. Fotina, V.L. Kravchuk, M. D'Agostino, L. Morelli, S. Ap-pannababu, G. Baiocco, S. Barlini, M. Bini, A. Brondi, M. Bruno, G. Casini, M. Cinausero, N. Gelli, R. Moro, A. Olmi, G. Pasquali, S. Piantelli, G. Poggi, S. Valdrè and E. Vardaci, Acta Phys. Pol. B**46**, 447 (2015).

[20] D. Fabris, F. Gramegna, M. Cicerchia, T. Marchi, S. Barlini, S. Piantelli, M. Bini, M. Bruno, G. Casini, M. Cinausero, M. D'Agostino, M. Degerlier, N. Gelli, G. Mantovani, L. Morelli, J. Mabiala, A. Olmi, G. Pasquali, G. Poggi, S. Valdrè, E. Vardaci, O.V. Fotina, V.L. Kravchuk, M. Colonna and A. Ono, EPJ Web Conf. **163**, 00016(2017).

[21] J.V. Pilcher, A.A. Cowley, J.J. Lawrie and D.M. Whittal, Phys. Rev. C **40**, 1937 (1989).

[22] G.D. Westfall, Z.M. Koenig, B.V. Jacak, L.H. Harwood, G.M. Crawley, C.K. Gelbke, B. Hasselquist, W.G. Lynch, A.D. Panagiotu, D.K. Scott, H. Stöcker and M.B. Tsang, Phys. Rev. C **29**, 861 (1984).

[23] B. Borderie, M.F. Rivet, I. Forest, J. Galin, D. Guerreau, R. Bimbot, D. Gardes, B. Gatty, M. Lefort, H. Oeschler, S. Song, B. Tamain and X. Tarrago, Nucl. Phys. A **402**, 57 (1983).